Kobe University Repository : Kernel

PDF issue: 2025-12-05

Decamethyl- and octamethyl-ferrocenium salts of F1- and F2-TCNQ: Effects of fluorine substitution on the crystal structures and magnetic interactions

Funasako, Yusuke ; Mochida, Tomoyuki ; Akasaka, Takahiro ; Sakurai, Takahiro ; Ohta, Hitoshi ; Nishio, Yutaka

---

(Citation)
Inorganica Chimica Acta,419:105-110

(Issue Date)
2014-05

(Resource Type)
journal article

(Version)
Accepted Manuscript

(URL)
https://hdl.handle.net/20.500.14094/90002538

Decamethyl- and octamethyl-ferrocenium salts of F_1- and F_2-TCNQ: Effects of fluorine substitution on the crystal structures and magnetic interactions

Yusuke Funasako[a], Tomoyuki Mochida[a]*, Takahiro Akasaka[a,b], Takahiro Sakurai[c], Hitoshi Ohta[d], Yutaka Nishio[e]

[a]*Department of Chemistry, Graduate School of Science, Kobe University, Kobe, Hyogo 657-8501, Japan*
[b]*Department of Chemistry, Faculty of Science, Toho University, Miyama, Funabashi, Chiba 274-8510, Japan*
[c]*Center for Supports to Research and Education Activities, Kobe University, Kobe, Hyogo 657-8501, Japan*
[d]*Molecular Photoscience Research Center, Kobe University, Kobe, Hyogo 657-8501, Japan*
[e]*Department of Physics, Faculty of Science, Toho University, Miyama, Funabashi, Chiba 274-8510, Japan*

ABSTRACT

Decamethyl- and octamethyl-ferrocenium salts of F_nTCNQ (n = 1, 2) were prepared and their crystal structures characterized. The 2,5-F_2TCNQ salts $[Fe(C_5Me_5)_2](2,5\text{-}F_2TCNQ)$ (**1**) and $[Fe(C_5Me_4H)_2](2,5\text{-}F_2TCNQ)$ (**2**) exhibit one-dimensional $...[D]^+[A]^-[D]^+[A]^-...$ mixed-stack structures, while the salts with polar acceptors $[Fe(C_5Me_5)_2][A]$ (A = F_1TCNQ (**3**), 2,3-F_2TCNQ (**4**), 2,6-F_2TCNQ (**5**)) and $[Fe(C_5Me_4H)_2][A]$ (A = 2,3-F_2TCNQ (**6**), 2,6-F_2TCNQ (**7**)) consist of $[D]^+[A_2]^{2-}[D]^+$ units involving a diamagnetic dimer of the acceptors. These salts are isomorphous to the corresponding TCNQ salts. **1** and **2** exhibit small ferromagnetic interactions at low temperatures. **1** undergoes an antiferromagnetic phase transition at T_N = 3.9 K, which is higher than T_N = 2.1 K of the metamagnetic polymorph of $[Fe(C_5Me_5)_2](TCNQ)$.

Keywords: Decamethylferrocene; F_nTCNQ; Crystal structures; Magnetic properties

---

*Corresponding author. Tel/fax: +81 78 803 5679.

E-mail address: tmochida@platinum.kobe-u.ac.jp (T. Mochida).

1. Introduction

Metallocene-based charge-transfer (CT) salts have attracted a lot of attention owing to their solid-state electronic properties such as magnetism and electrical conductivities [1,2]. One of the most notable examples is $[Fe(C_5Me_5)_2](TCNQ)$ (decamethylferrocenium 7,7,8,8-tetracyano-*p*-quinodimethanide), which has three polymorphs: the metamagnetic phase (T_N = 2.1 K), the ferromagnetic phase (T_C = 3.0 K), and the paramagnetic phase [3–8]. The former two polymorphs have a one-dimensional (1-D) mixed-stack structure ($...[D]^+[A]^-[D]^+[A]^-...$), whereas the latter is a "dimeric phase" polymorph consisting of $[D]^+[A_2]^{2-}[D]^+$ units involving a diamagnetic dimer of acceptors. Several related salts have been reported. $[Fe(C_5Me_4H)_2](TCNQ)$ ($[Fe(C_5Me_4H)_2]$ = octamethylferrocene) has a 1-D mixed-stack structure [9]. $[Fe(C_5Me_5)_2](F_4TCNQ)$ is isomorphous to the dimeric phase of $[Fe(C_5Me_5)_2](TCNQ)$ [10].

Our group recently investigated the effects of fluorine substituents on the assembled structures of alkylferrocenium salts of F_nTCNQ [11]. The packing structures of these salts were found to vary depending on the number of fluorine atoms. This approach is interesting from the viewpoint of crystal engineering [12]. In this study, $[Fe(C_5Me_5)_2](F_nTCNQ)$ and $[Fe(C_5Me_4H)_2](F_nTCNQ)$ (n = 1, 2) were prepared to examine the effects of the fluorine substituents (Fig. 1). The half-wave redox potentials ($E_{1/2}$ in CH_3CN, vs. SCE) of TCNQ, F_1TCNQ, and 2,5-F_2TCNQ are 0.22 V, 0.32 V, and 0.41 V, respectively [13], and their use for CT complexes are well documented [14]. 2,3- and 2,6-F_2TCNQ, which are polar isomers of 2,5-F_2TCNQ [14], were also used to investigate the effect of acceptor polarity. Herein, we report the preparation and crystal structures of the salts **1**–**7** shown in Fig. 2. The magnetic properties of **1** and **2** were also investigated.

2. Results and discussion

2.1. Preparation and general structural features

Determination of the crystal structures revealed that **1** and **2**, which are the salts of the centrosymmetric acceptor 2,5-F_2TCNQ, exhibit 1-D mixed-stack structures. They are isomorphous to [Fe(C_5Me_5)$_2$](TCNQ) (metamagnetic polymorph) and [Fe(C_5Me_4H)$_2$](TCNQ), respectively. In contrast, the salts with polar acceptors (**3**–**7**) were isomorphous to the dimeric phase polymorph of [Fe(C_5Me_5)$_2$](TCNQ) (Fig. 2). All of the salts exhibit a 1:1 donor/acceptor ratio, and the molecular geometries of the donors and acceptors are consistent with those of monocations and monoanions [15], respectively. We tried various crystallization conditions, but these phases were obtained exclusively as single crystals and no polymorphism was observed. It seems reasonable that the polar acceptors favoring dimer formation produce the dimeric phase structure. This is further supported by results of the examination of the acceptor arrangements (*vide infra*). There were no close Fe···NC- arrangements between the cation and anion, as observed in the ferrocenium salts of TCNQ [11] and [M(mnt)$_2$]$^-$ [16].

The unit cell volumes and intermolecular distances of **1**–**7** and related salts are listed in Table 1. The cell volume of **1** (704.9 Å^3, at 167 K) was 0.45% larger than that of the metamagnetic polymorph of [Fe(C_5Me_5)$_2$](TCNQ) (701.8 Å^3, at 167 K), and that of **3** (2798.3 Å^3, at 293 K) was 0.47% larger than that of the dimeric phase polymorph of [Fe(C_5Me_5)$_2$](TCNQ) (2785.1 Å^3, at 293 K). Therefore, the effect of fluorine substitution was found to be smaller than that of temperature change; the thermal expansion of **1** on increasing the temperature from 167 K (704.9 Å^3) to 296 K (720.1 Å^3) was 2.1%, and that of **3** on going from 173 K (2743.3 Å^3) to 293 K (2798.3 Å^3) was 2.0%.

*2.2. Crystal structures of mixed-stack salts **1** and **2***

The packing diagrams of [Fe(C_5Me_5)$_2$](2,5-F_2TCNQ) (**1**) and [Fe(C_5Me_4H)$_2$](2,5-F_2TCNQ) (**2**) are shown in Figs. 3a and 3b, respectively. The structures of **1** and **2** consisted of a 1-D ...[D][A][D][A]... alternate stacking. The molecular planes of the adjacent donor and acceptor moieties are canted with respect to each other in **2** due to the asymmetric structure of the donor. The donor–acceptor distance and Fe...Fe distance in the 1-D stacked structure of **1** (3.47 Å, 10.48 Å) is shorter than those in **2** (3.55 Å, 10.29 Å) owing to the lack of methyl groups (Fig. 3). These tendencies are also observed in the corresponding TCNQ salts [9].

The intermolecular Fe...Fe distances in the 1-D stacked structure of **1** (10.48 Å) and **2** (10.29 Å) are shorter by 0.07 Å than those of the corresponding salts with TCNQ (Table 1), whereas the interchain Fe...Fe distances are slightly longer. The acceptors form a ribbon structure along the *a*-axis, i.e., perpendicular to the stacking direction, via -CH···NC- hydrogen-bond-like contacts [17], which are shorter than the van der Waals distance by 0.2 Å (Fig. 4). This acceptor arrangement in **1** and **2** results in much shorter N···N distances between the acceptors (3.51 Å and 3.65 Å, respectively; Table 1) than those in the corresponding TCNQ salts (4.08 Å and 3.89 Å, respectively). This was the most prominent change in geometry caused by the fluorine substitution, which likely affects intermolecular magnetic interactions (*vide infra*). There are no significant intermolecular -CH···F- interactions.

*2.3. Crystal structures of dimeric phase salts **3**−**7***

$[Fe(C_5Me_5)_2][A]$ (A = F_1TCNQ (**3**), 2,3-F_2TCNQ (**4**), 2,6-F_2TCNQ (**5**)) and $[Fe(C_5Me_4H)_2][A]$ (A = 2,3-F_2TCNQ (**6**), 2,6-F_2TCNQ (**7**)) are isomorphous to the dimeric phase polymorph of $[Fe(C_5Me_5)_2]$(TCNQ), which consists of $[D][A]_2[D]$ units. The packing diagram of **3** is shown in Fig. 5. The C_5Me_5 rings of the cations in **3**–**5** that face away from the acceptor exhibit a twofold rotational disorder, where the occupancies of the dominant site are 0.8–0.9. The cations in **6**–**7** exhibit no disorder. There are -C_{Cp}H···F- short contacts between the donors and acceptors in **6** and **7**, which are 2.53 Å and 2.45 Å, respectively. The orientation of the acceptor, namely the position of the fluorine atom of F_1TCNQ, in **3** is disordered over two adjacent sites with an occupancy of 0.5:0.5; hence, its molecular shape appears similar to that of 2,3-F_2TCNQ. Similarly, the acceptor orientations in **5**–**7** are disordered with occupancies of 0.72:0.28 (**5**), 0.88:0.12 (**6**), and 0.53:0.47 (**7**), while 2,3-F_2TCNQ in **4** is ordered. The acceptors in the centrosymmetric dimer are slipped with respect to each other along the molecular short axis, and hence, the energies of the dimer differ depending on the acceptor orientations more significantly for 2,3-F_2TCNQ than for 2,6-F_2TCNQ

(Fig. 6). This is probably the reason why the disorder ratio of 2,3-F_2TCNQ exhibits a larger deviation from 0.5:0.5 than that of 2,6-F_2TCNQ.

It is to be noted that the interplane distances between the acceptors in the dimer (3.13–3.24 Å), the donor–acceptor interplane distances (3.69–3.75 Å), and the Fe...Fe distances in the $[D][A]_2[D]$ units (13.84–14.06 Å) vary slightly in these salts (Table 1). These distances in the F_1 and 2,3-F_2TCNQ salts are shorter than those in the 2,6-F_2TCNQ and TCNQ salts. This tendency indicates stronger intradimer interactions for the acceptors having larger transverse dipole moments, which is again reflective of acceptor polarity. The centroid–centroid distances between the acceptors are 3.241–3.254 Å (Table 1), and there was no correlation between the values and the substituent positions. The donor–acceptor interplane distances in the salts with $[Fe(C_5Me_5)_2]$ and $[Fe(C_5Me_4H)_2]$ are almost the same. This contrasts with the tendency observed for **1** and **2**.

*2.4. Magnetic properties of **1** and **2***

To investigate the effect of fluorine substitution on the magnetic transition of the metamagnetic polymorph of $[Fe(C_5Me_5)_2]$(TCNQ) [3a], we examined the magnetic property of the isomorphous salts **1**. The temperature dependence of the magnetic susceptibility (χT value) of **1** is shown in Fig. 7. The value at room temperature was 1.14 emu K mol^{-1}, which corresponds to the sum of the contribution by the decamethylferrocenium cation (~0.7 emu K mol^{-1}) and the F_2TCNQ anion (0.375 emu K mol^{-1}). In **1**, the value increased at temperatures below approximately 50 K, and the magnetic susceptibility (χ) exhibited a maximum at 4.5 K. This behavior closely resembles that of the metamagnetic polymorph of $[Fe(C_5Me_5)_2]$(TCNQ) [3]. The antiferromagnetic phase transition temperature (T_N) determined from the maximum of $d(\chi T)/dT$ was 3.9 K. The Weiss temperature (θ) estimated from the Curie–Weiss fitting was +1.6 K. The value was smaller than those of the metamagnetic and ferromagnetic polymorphs of $[Fe(C_5Me_5)_2]$(TCNQ), which are $\theta = +3$ K [4] and +3.8 K [7], respectively. The coercive field (H_C) at 2 K was determined to be 0.99 T from the magnetization curve (Fig. 7, inset). Specific heat measurements revealed the presence of an excess heat capacity that corresponds to the antiferromagnetic phase transition (Fig. 8). The transition temperature and transition entropy were determined to be T_N = 3.9 K and ΔS = 9.6 J mol^{-1} K^{-1}, respectively. The transition entropy is consistent with magnetic ordering, for which, a value of $2R \ln 2$ (11.5 J mol^{-1} K^{-1}) is expected.

Compared with the T_C of $[Fe(C_5Me_5)_2](TCNQ)$ (T_C = 2.1 K, H_C (2 K) = 0.13 T [3]), the T_C of **1** is higher by ~2 K and the H_C is about seven times larger, suggesting stronger intercolumn antiferromagnetic interactions in **1**. This is probably ascribed to the shorter N···N distances between the acceptors, which likely to transmit interchain magnetic interactions better [2a]. The values of T_N and H_C in $[Fe(C_5Me_5)_2](TCNQ)$ increase with pressure (T_C = 2.9 K and H_C (2 K) = 0.18 T, at 2.9 kbar) [3]. The lattice volume as well as the interchain distance are larger in **1** than in $[Fe(C_5Me_5)_2](TCNQ)$; hence, it was shown that the effect of fluorine substitution on the magnetic property is not a simple negative chemical pressure effect.

We also examined the magnetic properties of **2** (Fig. 9). The χT value at room temperature was 1.13 emu K mol^{-1}. The value increased with decreasing temperature below approximately 50 K, indicating the presence of ferromagnetic interactions (θ = +1.1 K). No magnetic phase transition was observed above 2 K. In contrast, $[Fe(C_5Me_4H)_2](TCNQ)$ exhibits antiferromagnetic interactions at low temperatures [9].

3. Conclusion

$[Fe(C_5Me_5)](F_nTCNQ)$ and $[Fe(C_5Me_4H)](F_nTCNQ)$ (n = 1 and 2) formed either the 1-D ...$[D]^+[A]^-[D]^+[A]^-$... mixed-stack structure or the dimeric phase structure consisting of $[D]^+[A_2]^{2-}[D]^+$ units although $[Fe(C_5Me_5)](TCNQ)$ adopts both the crystal phases. The assembled structures depended on the acceptor polarity; the nonpolar acceptor (2,5-F_2TCNQ) formed the former structure, while the polar acceptors (F_1TCNQ, 2,3-F_2TCNQ, and 2,6-F_2TCNQ) formed the latter structure. It seems reasonable that the polar acceptors form dimers in order to cancel their dipole moments to form the dimeric phase structure. The acceptor orientation, namely the position of the fluorine atoms, was disordered in most salts. The extent of disorder as well as the intermolecular distances in the salts depended on the acceptor polarity. The use of F_nTCNQ provides an effective method to investigate chemical pressure effects. However, it was demonstrated that the effect of fluorine on the magnetic interactions in $[Fe(C_5Me_5)](TCNQ)$ and $[Fe(C_5Me_4H)_2](TCNQ)$ were not due to simple expansion of the cell volume, but due to changes in the intermolecular arrangement.

4. Experimental

4.1. Materials and physical measurements

Decamethylferrocene and octamethylferrocene were purchased from Sigma-Aldrich and used after recrystallization from MeCN. F_nTCNQs were prepared according to literature methods [18]. FT-IR spectra were recorded as KBr pellets on a Thermo Nicolet Avatar 360 spectrometer. Magnetic susceptibilities were measured using a Quantum Design MPMS–2 SQUID susceptometer in the temperature range of 2–300 K under a field of 1000 G. Calorimetric measurements of single crystals were conducted using a thermal relaxation method. The sample was attached to a bolometer with Apiezon N grease. A sample holder made of Stycast 1266 was located in the mixing chamber of a dilution refrigerator, and a vacuum was created inside the holder using charcoal. It was possible to measure the specific heat over a wide range of temperatures from 0.2 to 9 K because the heat-contact of the thermal bath with a ^{3}He-^{4}He mixture in the mixing chamber was suppressed.

4.2. Syntheses

Single crystals of **1** and **2** were obtained by slow diffusion of chloroform solutions of the donor and the acceptor. Single crystals of **3**–**5** and **7** were obtained by diffusion of diethylether into acetonitrile solutions of the components, and those of **6** by slow cooling of acetonitrile solutions down to –40 °C. The use of different solvents (ex. acetonitrile for **1**) also produced the same crystal forms but resulted in poor quality. **1**: Yield 44%. 14.0 mg of **1** was obtained from 18.2 mg (0.06

mmol) of the donor and 13.5 mg (0.06 mmol) of the acceptor. IR: ν = 3045, 2185(CN), 2168, 1518, 1483, 1476, 1389, 1342, 1202, 1142, 1026, 901, 787. Anal. Calcd.for $C_{32}H_{32}F_2FeN_4$ (566.47): C, 67.85; H, 5.69; N, 9.89. Found: C, 67.74; H, 5.67; N, 9.91. **2**: Yield 25%. 14.2 mg of **2** was obtained from 31.5 mg of the donor and 25.2 mg of the acceptor. IR (cm^{-1}): ν = 3075, 3055, 2183 (CN), 2166 (CN), 2127 (CN), 1547, 1516, 1483, 1454, 1414, 1391, 1373, 1341, 1296, 1202, 1165, 1150, 1138, 1028, 887, 787. Anal. Calcd.for $C_{30}H_{28}F_2FeN_4$ (538.41): C, 66.92; H, 5.24; N, 10.41. Found: C, 66.55; H, 5.13; N, 10.61. **3**: Yield 55%. 15 mg of **3** was obtained from 15 mg of the donor and 11 mg of the acceptor. IR: ν = 2920, 2181 (CN), 2168 (CN), 1603, 1514, 1491, 1450, 1423, 1387, 1368, 1325, 1256, 1186, 1119, 1074, 1020, 982, 866, 818. Anal. Calcd.for $C_{32}H_{33}FFeN_4$ (548.47): C, 70.07; H, 6.06; N, 10.22. Found: C, 69.87; H, 6.06; N, 10.34. **4**: Yield 76%. 9 mg of **4** was obtained from 8 mg of the donor and 5 mg of the acceptor. ν (cm^{-1}) = 2903, 2184 (CN), 2171 (CN), 1613, 1510, 1483, 1423, 1377, 1328, 1218, 1190, 1085, 1021, 873, 808, 722, 617, 592. Anal. Calcd.for $C_{32}H_{32}F_2FeN_4$ (566.47): C, 67.85; H, 5.69; N, 9.89. Found: C, 67.63; H, 5.90; N, 9.62. **5**: Yield 17%. 4 mg of **5** was obtained from 15 mg of the donor and 10 mg of the acceptor. ν (cm^{-1}) = 2916, 2183 (CN), 2179 (CN), 1611, 1516, 1499, 1388, 1370, 1324, 1220, 1175, 1019, 848, 796, 712, 612, 596. Anal. Calcd.for $C_{32}H_{32}F_2FeN_4$ (566.47): C, 67.85; H, 5.69; N, 9.89. Found: C, 66.78; H, 5.68; N, 9.69. **6**: Yield 95%. 17 mg of **6** was obtained from 12 mg of the donor and 8 mg of the acceptor. ν (cm^{-1}) = 3078, 2921, 2184 (CN), 2171 (CN), 1611, 1510, 1487, 1377, 1325, 1218, 1191, 1086, 1022, 980, 874, 807, 722, 618, 609. Anal. Calcd.for $C_{30}H_{28}F_2FeN_4$ (538.41): C, 66.92; H, 5.24; N, 10.41. Found: C, 67.10; H, 5.26; N, 10.42. **7**: Yield 99%. 18 mg of **7** was obtained from 12 mg of the donor and 8 mg of the acceptor. ν (cm^{-1}) = 3081, 2920, 2184 (CN), 2173 (CN), 1610, 1515, 1498, 1388, 1364, 1323, 1236, 1220, 1204, 1175, 1041, 1020, 987, 848, 838, 712, 609, 596. Anal. Calcd.for $C_{30}H_{28}F_2FeN_4$ (538.41): C, 66.92; H, 5.24; N, 10.41. Found: C, 66.94; H, 5.26; N, 10.61.

4.3. X-ray crystal structure determination

X-ray diffraction data for single crystals were collected on a Bruker SMART APEX II CCD diffractometer using Mo K*α* radiation (*λ* = 0.71073 Å). Their crystallographic parameters are listed in Tables 2 and 3. All calculations were performed using SHELXL [19]. The non-hydrogen atoms were refined anisotropically. Empirical absorption corrections were applied. The hydrogen atoms were inserted at the calculated positions and allowed to ride on their respective parent atoms. ORTEP-3 [20] was used to generate molecular graphics.

Acknowledgments

This work was financially supported by KAKENHI (grant number 23110719). We thank Dr. Y. Furuie (Kobe University) for elemental analysis and Ms. Michiko Sato (Toho University) for her help with specific heat measurements.

Appendix A. Supplementary material

CCDC 942506 (**1**), 942507 (**2**), 942508 (**3**), 951723(**4**), 951724 (**5**), 953082 (**6**), and 953083 (**7**) contain the supplementary crystallographic data. These data can be obtained free of charge via http://www.ccdc.cam.ac.uk/data-request/cif.

References

[1] (a) Ferrocenes: Homogenous Catalysis, Organic Synthesis, Materials Science, A. Togni, T. Hayashi, Eds. Wiley–VCH, Weinheim (1995) Chapter 8. (b) N.J. Long, Metallocenes: an introduction to sandwich complexes, Blackwell Science, Oxford (1998).

[2] (a) J.S. Miller, J. Mat. Chem. 20 (2010) 1846–1857; (b) J.S. Miller, A.J. Epstein, W.M. Reiff, Angew. Chem. Int. Ed. Engl. 33 (1994) 385–415; (c) S. Zürcher, S.J. Petrig, V. Gramlich, M. Worle, C. Mensing, D. von Arx, A. Togni, Organometallics 18 (1999) 3679–3689; (d) C. Faulmann, P. Cassoux, Prog. Inorg. Chem. 52 (2004) 399–489.

[3] (a) J.G. DaSilva, J.S. Miller, Inorg. Chem. 52 (2013) 1108–1112; (b) M.L. Taliaferro, F. Palacio, J.S. Miller, J. Mat. Chem. 16 (2006) 2677–2684.

[4] J.S. Miller, J.H. Zhang, W.M. Reiff, D.A. Dixon, L.D. Preston, A.H. Reis, Jr., E. Gebert, M. Extine, J. Troup, A.J. Epstein, M.D. Ward, J. Phys. Chem. 91 (1987) 4344–4360.

[5] G.A. Candela, L.J. Swartzendruber, J.S. Miller, M.J. Rice, J. Am. Chem. Soc. 101 (1979) 2755–2756.

[6] A.H. Reis, L.D. Preston, J.M. Williams, S.W. Pesterson, G.A. Candela, L.J. Swartzendruber, J.S. Miller, J. Am. Chem. Soc. 101 (1979) 2756–2758.

[7] W.E. Broderick, D.M. Eichhorn, X.Liu, P.J. Toscano, S.M. Owens, B.M. Hoffman, J. Am. Chem. Soc. 117 (1995) 3641–3642.

[8] M. Nakano, M. Sorai, Chem. Phys. Lett. 169 (1990) 27–30.

[9] J.S. Miller, D.T. Glatzhofer, D.M. O'Hare, W.M. Reiff, A. Chakraborty, A.J. Epstein, Inorg. Chem. 28 (1989) 2930–2939.

[10] D.A. Dixon, J.C. Calabrese, J.S. Miller, J. Phys. Chem. 93 (1989) 2284–2291.

[11] (a) T. Mochida, T. Akasaka, Y. Funasako, Y. Nishio, H. Mori, Cryst. Growth & Des. 13 (2013) 4460–4468; (b) T. Mochida, Y. Funasako, E. Nagabuchi, H. Mori, Cryst. Growth & Des. 14 (2014) 1459–1466.

[12] C.B. Aakeröy, N.R. Champness, C. Janiak, CrystEngComm 12 (2010) 22–43.

[13] S.-S. Pac, G. Saito, J. Solid State Chem. 168 (2002) 486–496.

[14] (a) T. Hasegawa, K. Inukai, S. Kagoshima, T. Sugawara, T. Mochida, S. Sugiura, Y. Iwasa, Chem. Commun. (1997) 1377–1378; (b) T. Hasegawa, S. Kagoshima, T. Mochida, S. Sugiura, Y. Iwasa, Solid State Commun. 103 (1997) 489–493.

[15] T.J. Kistenmacher, T.J. Emge, A.N. Bloch, D.O. Cowan, Acta Cryst. B38 (1982) 1193–1199.

[16] T. Mochida, T. Koinuma, T. Akasaka, M. Sato, Y. Nishio, K. Kajita, H. Mori, Chem. Eur. -J. 13 (2007) 1872–1881.

[17] G.R. Desiraju, Acc. Chem. Res. 35 (2002) 656–573.

[18] (a) T. Mochida, H. Moriyama, T. Hasegawa, R. Kondo, S. Kagoshima, Y. Iwasa, Synth. Met. 86 (1999) 1678–1679; (b) T. Mochida, T. Hasegawa, S. Kagoshima, S. Sugiura, Y. Iwasa,

Synth. Met. 86 (1997) 1797–1798.

[19] (a) G.M. Sheldrick, SHELXL, Program for the Solution of Crystal Structures; University of Göttingen: Göttingen, Germany, 1997. (b) G.M. Sheldrick, Acta Crystallogr. D64 (2008) 112–122.

[20] ORTEP-3 for Windows: L.J. Farrugia, J. Appl. Cryst. 30 (1997) 565.

Highlights

$[Fe(C_5Me_4R)_2](F_nTCNQ)$ (R = H, Me; $n = 1, 2$) are isomorphous to the TCNQ salts.

$[Fe(C_5Me_5)_2](2,5\text{-}F_2TCNQ)$ is a metamagnet with $T_N = 3.9$ K.

Polar acceptors (F_1-, 2,3-F_2-, and 2,6-F_2-TCNQ) form diamagnetic dimers in the salts.

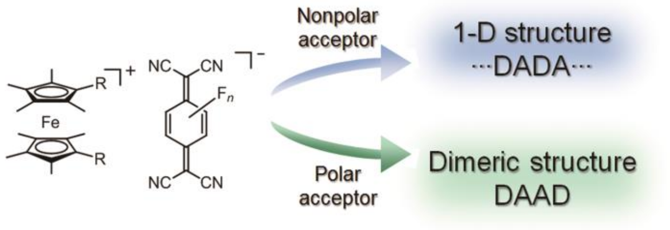

Table 1

Unit cell volumes and intermolecular distances in **1**–**7** and related compounds.

compounds	V (Å^3)	D–A (Å)[a]	A–A (Å)[a]	A–A (Å)[b]	Fe...Fe (Å)		N...N (Å)[c]	temp. (K)[d]
one-dimensional phase								
[Fe(C_5Me_5)](2,5-F_2TCNQ) (**1**)	704.9	3.540			10.482[e]	8.826[f]	3.514	167
[Fe(C_5Me_4H)$_2$](2,5-F_2TCNQ) (**2**)	638.0	3.473			10.288[e]	8.659[f]	3.653	173
[Fe(C_5Me_5)](TCNQ)[h,i]	701.8	3.567			10.55[e]	8.635[f]	4.080	167
[Fe(C_5Me_4H)$_2$](TCNQ)[j]	651.6	3.478			10.36[e]	8.636[f]	3.893	296
dimeric phase								
[Fe(C_5Me_5)](F_1TCNQ) (**3**)	2743.3	3.704	3.254	3.129	13.859[g]			173
[Fe(C_5Me_5)](2,3-F_2TCNQ) (**4**)	2783.2	3.695	3.241	3.136	13.843[g]			173
[Fe(C_5Me_5)](2,6-F_2TCNQ) (**5**)	2775.3	3.748	3.250	3.170	13.951[g]			173
[Fe(C_5Me_4H)$_2$](2,3-F_2TCNQ) (**6**)	2612.0	3.686	3.241	3.199	13.896[g]			173
[Fe(C_5Me_4H)$_2$](2,6-F_2TCNQ) (**7**)	2618.9	3.804	3.248	3.243	14.064[g]			173
[Fe(C_5Me_5)](TCNQ)[h]	2785.1	3.741	3.305	3.149	13.993[g]			rt
[Fe(C_5Me_5)](F_4TCNQ)[k]	2878.3							rt

[a] Distance between the centroids of adjacent rings.

[b] Acceptor–acceptor interplane distances in the acceptor dimer.

[c] The closest intermolecular N...N distance between adjacent acceptor molecules.

[d] The temperature at which the unit cell volume was determined.

[e] Intrachain Fe...Fe distance.

[f] In-registry interchain Fe...Fe distance. See Ref. 7 for definition.

[g] Intermolecular Fe...Fe distances in the DAAD unit.

[h] Metamagnetic polymorph.

[i] Ref. 4.

[j] Ref. 8.

[k] Ref. 9.

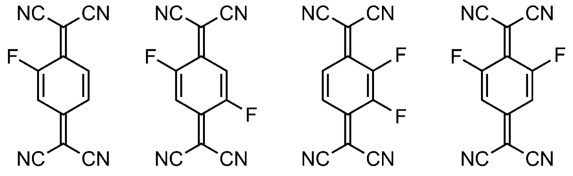

F_1TCNQ　2,5-F_2TCNQ　2,3-F_2TCNQ　2,6-F_2TCNQ

Fig. 1. Acceptors used in this study.

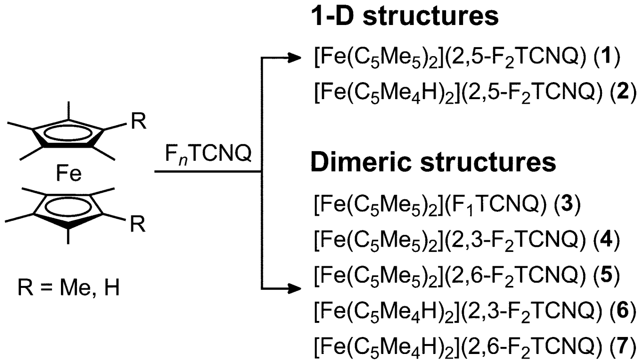

Fig. 2. General reaction scheme.

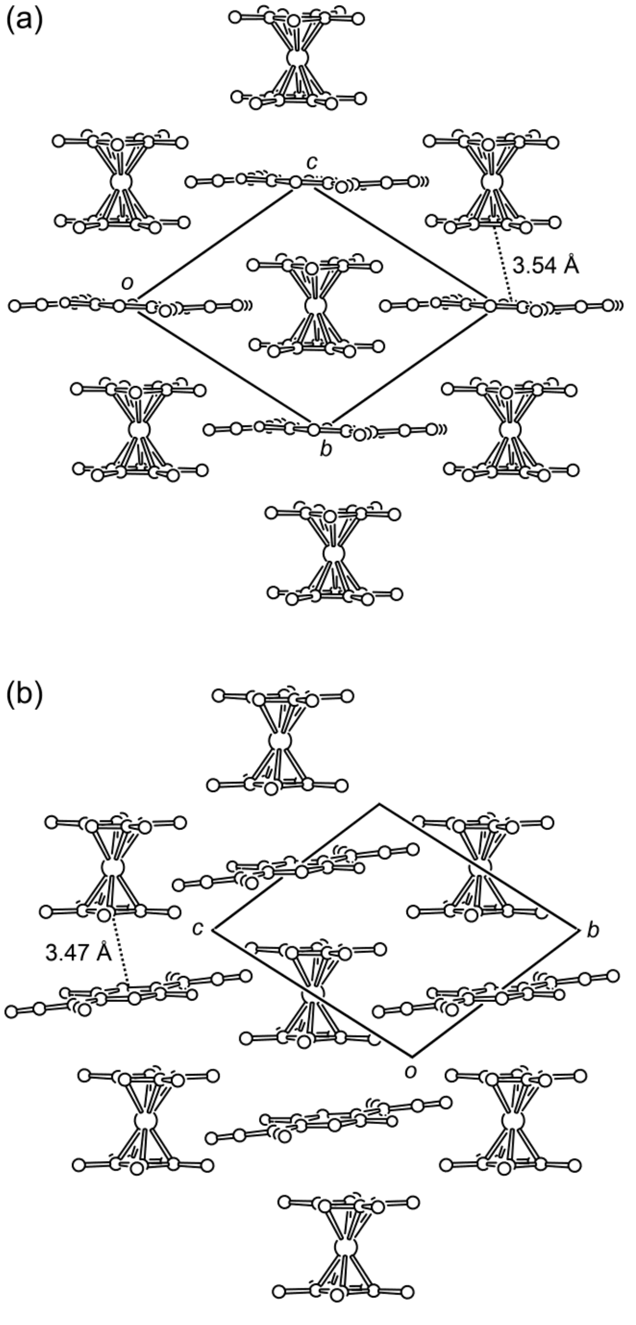

Fig. 3. Packing diagrams of a) [Fe(C_5Me_5)$_2$](2,5-F_2TCNQ) (**1**) and b) [Fe(C_5Me_4H)$_2$](2,5-F_2TCNQ) (**2**) projected along the *a*-axis.

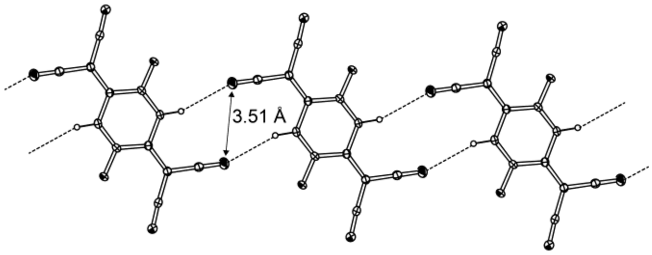

Fig. 4. The arrangement of the acceptors in [Fe(C_5Me_5)$_2$](2,5-F_2TCNQ) (**1**) arranged along the *a*-axis. Dotted lines indicate intermolecular contacts shorter than the van der Waals distances by 0.2 Å.

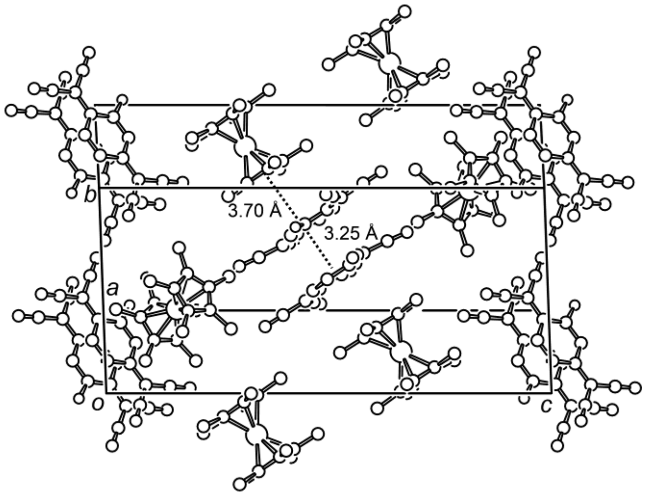

Fig. 5. Packing diagrams of [Fe(C_5Me_5)$_2$](F_1TCNQ) (**3**). The C_5Me_5 rings and fluorine atoms are disordered, and the disordered components are partly omitted.

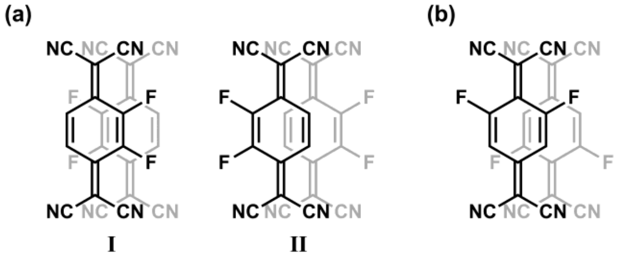

Fig. 6. The acceptor arrangements in the dimers of (a) 2,3-F_2TCNQ and (b) 2,6-F_2TCNQ. Form I was the dominant orientation in [Fe(C_5Me_5)$_2$](2,3-F_2TCNQ)$_2$ (**4**) and [Fe(C_5Me_4H)$_2$](2,3-F_2TCNQ)$_2$ (**6**).

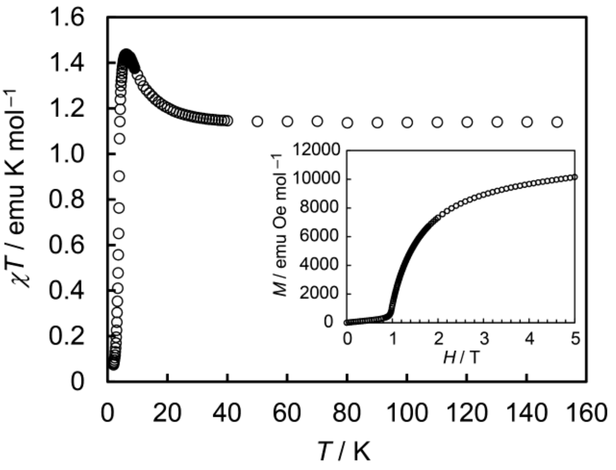

Fig. 7. Temperature dependence of the magnetic susceptibility (χT value) of $[Fe(C_5Me_5)_2](2,5\text{-}F_2TCNQ)$ (**1**). The inset shows the magnetization curve for **1** at 2 K.

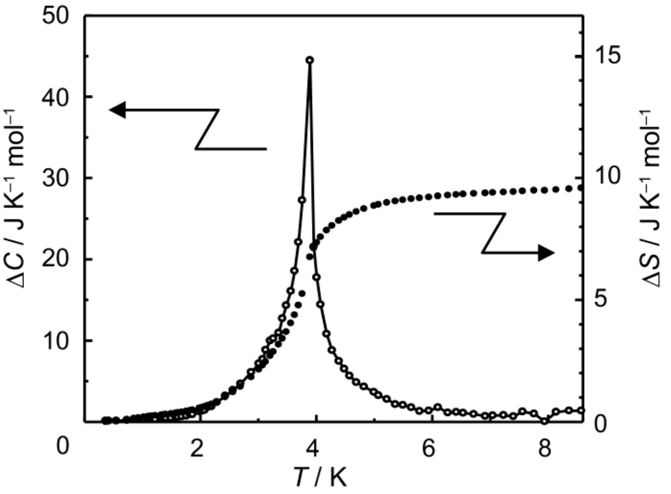

Fig. 8. Excess heat capacity and excess entropy of $[Fe(C_5Me_5)_2](2,5\text{-}F_2TCNQ)$ (**1**).

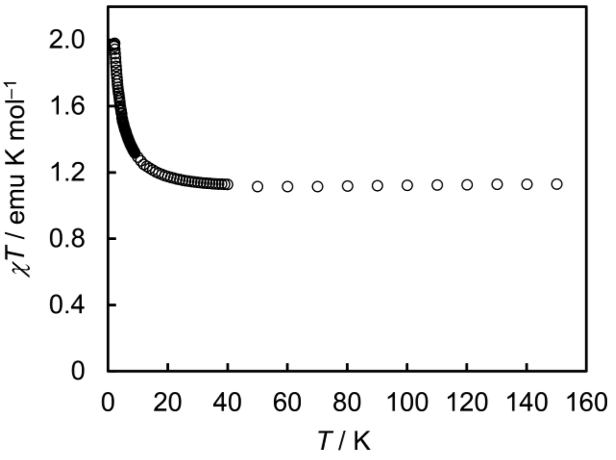

Fig. 9. Temperature dependence of the magnetic susceptibility (χT value) of $[Fe(C_5Me_4H)_2](2,5\text{-}F_2TCNQ)$ (**2**).